Structural Investigation of Solute−Solute Interactions in Aqueous Solutions of Tertiary Butanol

D. T. Bowron, J. L. Finney,* and A. K. Soper†

Department of Physics and Astronomy, University College London, Gower Street, London, WC1E 6BT, U.K.

Received: August 26, 1997; In Final Form: February 10, 1998

Hydrogen/deuterium isotopic substitution neutron diffraction techniques have been used to measure the solute−solute intermolecular structural correlations in 0.06, 0.11, and 0.16 mole fraction tertiary butanol−water solutions. Empirical potential structure refinement (EPSR) procedures have been used to extract detailed information relating to the intermolecular structure in these systems. A trend from hydrophobic to hydrophilic character of the solute−solute correlations as a function of solute concentration is observed. Of particular note is the domination of nonpolar to nonpolar solute contacts at 0.06 mole fraction concentration compared with a more complex mixture of nonpolar and polar solute−solute intermolecular contact configurations at the higher alcohol concentration.

I. Introduction

Alcohol−water mixtures are an important class of solvent media used in many chemical and biochemical processes. It has been often noted that the physical chemistry of these solutions is particularly interesting,[1] a direct result of the balance between the complex mixture of intermolecular interactions that occur between the amphiphilic alcohols and hydrophilic water molecules. Studies of the thermodynamics of these solutions have established that the intermolecular structure in these mixtures plays an important role since this structure is governed by the aforementioned balance of intermolecular forces. A general conclusion in the literature on these systems is that at low concentrations the properties of these solutions are determined by the alkyl residue in preference to the hydrogen bonding between the molecular species;[2] that is, hydrophobic hydration and the hydrophobic interaction are believed to dominate the physicochemical properties.

The miscibility of alcohols in water decreases with increasing solute size, and tertiary butanol is the largest alcohol molecule in the series that is fully miscible with water in all proportions. It is consequently considered to be the most hydrophobic of the lower water-soluble alcohols. This general degree of hydrophobicity is clearly seen in the thermodynamic properties of its aqueous solutions,[1] for example in the sharp minimum that occurs in the partial molar volume and corresponding maximum in the partial molar specific heat, $C_{P,2}$ at 0.04 mole fraction tertiary butanol in water. This system thus makes an ideal candidate for investigation of the structural properties commonly associated with hydrophobic effects.

An understanding of these hydrophobic effects is particularly relevant in many important areas of chemical, biological, and physical science, and while conventional theories attribute the origin of these aqueous solution phenomena to subtle structural correlations between the aqueous environment and the nonpolar solute moieties,[3] to date, a detailed understanding of the mechanisms involved remains elusive. This situation is largely due to a dearth of direct experimental evidence relating to the intermolecular structure in appropriate solute−solvent systems.

Improvements in experimental techniques, for example, isotopic substitution neutron scattering methods, are now beginning to allow us to address this unsatisfactory state of affairs. Here we present a detailed study of the intermolecular structure in aqueous solutions of tertiary butanol using neutron diffraction with H/D isotopic substitution and the newly developed method of empirical potential structure refinement (EPSR)[6] to outline a structural model for these solutions that is consistent with the experimental data. Tertiary butanol−water mixtures at 0.06, 0.11, and 0.16 mole fraction were chosen for study, the first concentration falling as close as technically feasible for the H/D substitution technique to the 0.04 mole fraction concentration at which the most striking features in the thermodynamic properties are evident, while the highest concentration corresponds to a solution in which the intermolecular interactions between alcohol molecules are more prevalent and the thermodynamic parameters are stable and largely comparable with those of the pure liquid alcohol. The intermediate concentration falls at a point where the thermodynamic parameters indicate the system to be transitional between the hydrophobic low concentration regime and the largely alcohol-like higher concentrations.

Neutron diffraction using isotopic labeling is now sufficiently powerful to allow for the direct measurement of intermolecular structure in suitable systems. Through the use of difference techniques applied to binary molecular systems, the data taken from chemically identical but isotopically distinct samples make it possible to extract the three intermolecular structural correlations of importance: the solute−solute, solvent−solvent, and solute−solvent terms. In the study presented here, the intermolecular liquid structure in the tertiary butanol solutions is investigated primarily through the solute−solute function. Later studies will discuss the water structure and water−solute interactions in these systems.

II. Experiment

The solute−solute intermolecular correlation functions in tertiary butanol−water mixtures were extracted using the hydrogen/deuterium isotopic substitution neutron scattering technique. Measurements of the neutron scattering from three isotopic analogues of alcohol in water were made at each of three concentrations. The isotopic compositions of the mixtures were

$$(CH_3)_3COH \text{ in } D_2O$$

$$(CD_3)_3COD \text{ in } D_2O \text{ (+ a small quantity of } H_2O)$$

* Corresponding author.

† Also at: ISIS Facility, Rutherford Appleton Laboratory, Chilton, Didcot, Oxon, OX11 0QX, U.K.

S1089-5647(97)02780-6 CCC: $15.00
Published on Web 04/11/1998

1:1 mixture of the above two solutions

The solution concentrations used in this study were 0.057, 0.1071, and 0.167 mole fraction alcohol in water, concentrations which correspond to alcohol/water molecular ratios of approximately 1:17, 1:8, and 1:5, respectively. The magnitude of the solute−solute correlation function when probed by the isotopic substitution neutron scattering technique is proportional to the square of the concentration of the isotopically exchanged atomic species. Consequently ≈0.06 mole fraction is the practical low concentration limit for second-order difference studies of this system given current neutron scattering facilities and instruments.

The small quantity of H_2O was added to the second isotopic mixture to correct for in-solution isotopic exchange between the hydrogen/deuterium sites on the water molecules and the hydrogen/deuterium site on the alcohol hydroxyl group. The hydrogen and deuterium atoms associated with the alcohol methyl group sites do not undergo in-solution isotopic exchange. For the purposes of the experiment, the samples were contained in flat cells constructed from TiZr alloy with a composition chosen so as to produce zero coherent scattering contribution to the measured diffraction. These cells had internal dimensions of 2 mm × 35 mm × 35 mm and were mounted such that the sample was oriented perpendicular to the incident neutron beam. The cells were maintained at ambient temperature (≈25 °C) and pressure (≈1 bar). Once collected, the diffraction data for each solution were corrected for absorption and multiple scattering and normalized to vanadium using the ATLAS programs,[4] and the corrections for inelastic scattering effects were performed by the procedure outlined in ref 5 by Soper and Luzar. The atomic densities of the three solutions were determined to be ≈0.1 atom $Å^{-3}$ from measurements of the mass of a known volume of hydrogenated tertiary butanol in H_2O. The neutron diffraction experiments were performed at the ISIS pulsed neutron source, Rutherford Appleton Laboratory, U.K., using the SANDALS diffractometer. This instrument is optimized for measurements on liquid systems containing significant quantities of light atoms such as hydrogen.

III. Theory

A. Isotopic Substitution Neutron Scattering. In a single neutron scattering experiment, the quantity obtained after the data have been corrected for experimental details such as absorption and multiple scattering of neutrons, the background scattering from the sample cell, and the self-scattering and inelasticity effects is the total structure factor $F(Q)$. This is defined as

$$F(Q) = \sum_{\alpha\beta} c_\alpha c_\beta b_\alpha b_\beta (S_{\alpha\beta}(Q) - 1) \tag{1}$$

where c_α and c_β are the atomic fractions of species α and β, respectively, while b_α and b_β are their coherent neutron scattering lengths. The summation is over all atom pairs in the sample, and $S_{\alpha\beta}(Q)$ are the partial structure factors that result from interatomic correlations between atom pairs α and β. Q, the magnitude of the momentum transfer vector of the scattered neutrons, is defined as $4\pi(\sin\theta/\lambda)$, where 2θ is the scattering angle and λ is the wavelength of the incident neutron. These partial structure factors are related to the partial pair distribution functions $g_{\alpha\beta}(r)$ by the mathematical relation

$$S_{\alpha\beta}(Q) - 1 = 4\pi\rho \int r^2 [g_{\alpha\beta}(r) - 1] \frac{\sin(Qr)}{Qr}\, dr \tag{2}$$

where ρ is the average atomic number density of the sample.

Through the use of isotopes of differing coherent neutron scattering lengths, it is possible to extract some of the partial structure factors and less complex composite partial structure factors from the total structure factor of eq 1. Provided that the interatomic and intermolecular structure of an isotopically enhanced sample is to first order identical, this is a reliable technique.

In the case of a second-order difference hydrogen/deuterium isotopic substitution experiment the total structure factor, $F(Q)$, can be written as consisting of three terms, $S_{XX}(Q)$, $S_{XH}(Q)$, and $S_{HH}(Q)$ (eq 3). The label H refers to substituted atoms in the sample and X to unsubstituted atomic species.

$$F(Q) = c_X^{\,2} b_X^{\,2} [S_{XX}(Q) - 1] + 2c_X c_H b_X b_H [S_{XH}(Q) - 1] + c_H^{\,2} b_H^{\,2} [S_{HH}(Q) - 1] \tag{3}$$

The composite coherent scattering length, b_X, and concentration, c_X, are defined as

$$b_X = \sum_{\alpha \neq H} \frac{c_\alpha b_\alpha}{c_X} \tag{4}$$

$$c_X = \sum_{\alpha \neq H} c_\alpha \tag{5}$$

Consequently $c_H = (1 - c_X)$, and the $S_{HH}(Q)$ term in eq 3 is calculated from

$$S_{HH}(Q) - 1 = \frac{xF_H(Q) + (1-x)F_D(Q) - F_{HD}(Q)}{c_H^{\,2}(x b_H^{\,2} + (1-x) b_D^{\,2} - b_{HD}^{\,2})} \tag{6}$$

where the subscripts H and D refer to the experiments on the hydrogenated and deuterated samples, respectively, and HD refers to the mixture sample. x is the fraction of light hydrogen in the mixture sample, and thus

$$b_{HD} = x b_H + (1 - x) b_D \tag{7}$$

From an experimental viewpoint, it should be noted that the maximum difference between the scattering functions can be obtained if the three experiments performed for the second-order difference calculation use two pure isotopic compositions and a 1:1 mixture for the third.

The weighted sums for the other partial structure factors in eq 3, i.e. those that involve unlabeled atoms, are

$$(S_{XH}(Q) - 1) = \sum_{\alpha \neq H} \frac{c_\alpha b_\alpha (S_{\alpha H}(Q) - 1)}{c_X b_X} \tag{8}$$

$$(S_{XX}(Q) - 1) = \sum_{\alpha \neq H, \beta \neq H} \frac{c_\alpha c_\beta b_\alpha b_\beta (S_{\alpha\beta}(Q) - 1)}{c_X^{\,2} b_X^{\,2}} \tag{9}$$

and these composite partial structure factors can be calculated in a fashion similar to $(S_{HH}(Q) - 1)$ as

$$S_{XH}(Q) - 1 = \frac{F_H(Q) - F_D(Q) - c_H^{\,2} b_H^{\,2} (S_{HH}(Q) - 1) + c_H^{\,2} b_D^{\,2} (S_{HH}(Q) - 1)}{(2c_H c_X b_H b_X - 2c_H c_X b_D b_X)} \tag{10}$$

and

$$S_{XX}(Q) - 1 = \frac{F_H(Q) - 2c_Hc_Xb_Hb_X(S_{XH}(Q) - 1) - c_H^2b_H^2(S_{HH}(Q) - 1)}{c_X^2b_X^2} \quad (11)$$

Using the Fourier transform relationship complementary to that shown in eq 2, the partial structure factors between atom sites, $g_{\alpha\beta}(r)$, can be calculated. The positions of the features in $g_{HH}(r)$ correspond to interatomic distance correlations between substituted hydrogen sites. The area under these features is related to coordination numbers, the coordination number of atoms of type β at a distance between r_1 and r_2 from atoms of type α being defined as

$$(N_\beta^{(\alpha)})_{r_1}^{r_2} = 4\pi\rho c_\beta \int_{r_1}^{r_2} r^2 g_{\alpha\beta}(r)\, dr \quad (12)$$

B. Data Modeling and Spherical Harmonic Reconstruction. To make full use of the measured individual and composite partial structure factor information, some form of data modeling is required. Here we apply the newly developed technique of empirical potential structure refinement (EPSR).[6] In this technique an assumption is made that all the atoms or molecules interact by purely pairwise forces, and within this constraint, it is known that a unique relationship between the pair potential $U_{\alpha\beta}(r)$ and the pair correlation function $g_{\alpha\beta}(r)$ exists. In systems where many-body effects are important, progress can be made through the use of effective pair potentials which account for these many-body interactions as an average. These effective potentials can thus be used to determine pair correlation functions.

In the EPSR method, a set of experimentally determined pair correlation data $g_{\alpha\beta}^D(r)$ are used to constrain a Monte Carlo simulation. The method is based upon the development of a potential of mean force $\psi_{\alpha\beta}(r)$ between atoms α and β. This is defined as

$$\psi_{\alpha\beta}(r) = -kT \ln(g_{\alpha\beta}(r)) \quad (13)$$

The procedure for the modeling of the data begins with the establishment of a model fluid with the correct density and temperature, and using assumed potentials $U_{\alpha\beta}^O(r)$ between sites α and β. If this fluid consists of molecules, the basic structure of these units must also be constrained during the simulation. From this model fluid an estimate of the pair distribution function $g_{\alpha\beta}(r)$ can be made and a new potential energy function $U_{\alpha\beta}^N(r)$ can be estimated from the assumed potential

$$U_{\alpha\beta}^N(r) = U_{\alpha\beta}^O(r) + (\psi_{\alpha\beta}^D(r) - \psi_{\alpha\beta}(r)) = U_{\alpha\beta}^O(r) + kT\left(\ln\left(\frac{g_{\alpha\beta}(r)}{g_{\alpha\beta}^D(r)}\right)\right) \quad (14)$$

This new potential is then fed back into the simulation, and particles within the simulation box are moved. This process of evaluating a new potential is repeated periodically after a series of particle moves until such a time when

$$U_{\alpha\beta}^O(r) \approx U_{\alpha\beta}^N(r) \quad (15)$$

and hence

$$g_{\alpha\beta}(r) \approx g_{\alpha\beta}^D(r) \quad (16)$$

for all r and all pairs of atoms.

TABLE 1: Intermolecular Weightings on the Contributions to the X−X and X−M Experimentally Determined Composite Partial Structure Factors

X−X	conc	CC	C	O	H	OW	HW
CC	0.06	0.0004					
	0.11	0.0013					
	0.16	0.0027					
C	0.06	0.0025	0.0037				
	0.11	0.0079	0.0118				
	0.16	0.0159	0.0239				
O	0.06	0.0007	0.0021	0.0003			
	0.11	0.0023	0.0069	0.0010			
	0.16	0.0046	0.0139	0.0020			
H	0.06	0.0008	0.0023	0.0007	0.0004		
	0.11	0.0024	0.0072	0.0021	0.0011		
	0.16	0.0046	0.0138	0.0040	0.0020		
OW	0.06	0.0112	0.0336	0.0098	0.0107	0.0767	
	0.11	0.0186	0.0557	0.0162	0.0169	0.0656	
	0.16	0.0243	0.0730	0.0212	0.0211	0.0558	
HW	0.06	0.0245	0.0735	0.0214	0.0234	0.3351	0.3663
	0.11	0.0387	0.1161	0.0338	0.0353	0.2737	0.2855
	0.16	0.0482	0.1447	0.0421	0.0418	0.2212	0.2193

X−M	conc	CC	C	O	H	OW	HW
M	0.06	0.0202	0.0607	0.0177	0.0193	0.2769	0.6052
	0.11	0.0362	0.1087	0.0317	0.0330	0.2561	0.5343
	0.16	0.0515	0.1545	0.0450	0.0446	0.2362	0.4683

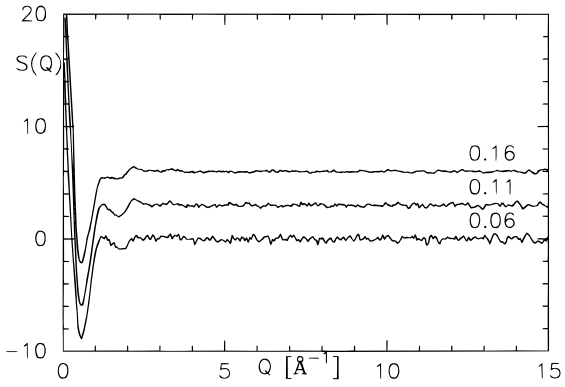

Figure 1. Partial structure factors $S_{HH}(Q)$ for 0.06 (bottom), 0.11 (middle), and 0.16 (top) mole fraction tertiary butanol in water. These functions have been offset vertically for clarity.

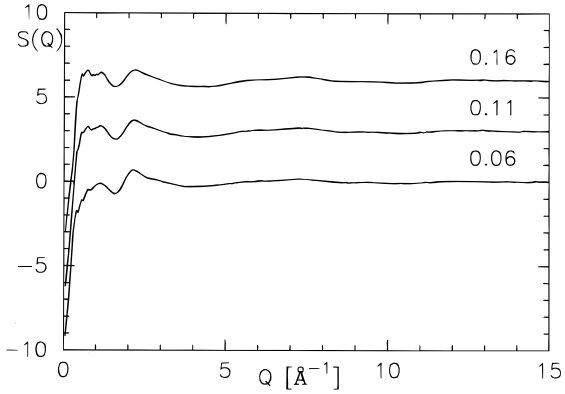

Figure 2. Partial structure factors $S_{XH}(Q)$ for 0.06 (bottom), 0.11 (middle), and 0.16 (top) mole fraction tertiary butanol in water. These function have been offset vertically for clarity.

Once the system model has reached an equilibrium configuration such that it satisfies eq 16, the Monte Carlo modeling process is continued and an ensemble of satisfactory intermolecular configurations is generated. This ensemble can then be analyzed to determine ensemble-averaged site−site radial distribution functions and, for molecular systems, the intermolecular orientational pair correlation function, $g(\mathbf{r},\omega_1,\omega_2)$. The

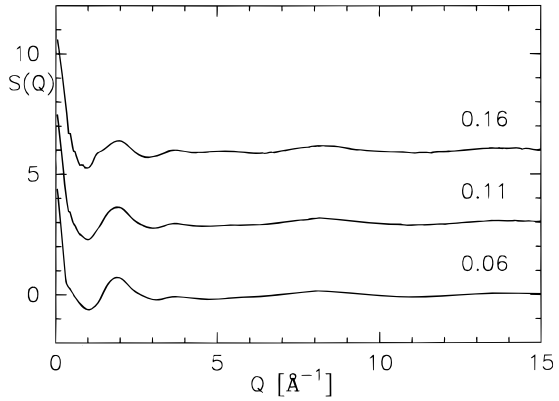

Figure 3. Partial structure factors $S_{XX}(Q)$ for 0.06 (bottom), 0.11 (middle), and 0.16 (top) mole fraction tertiary butanol in water. These functions have been offset vertically for clarity.

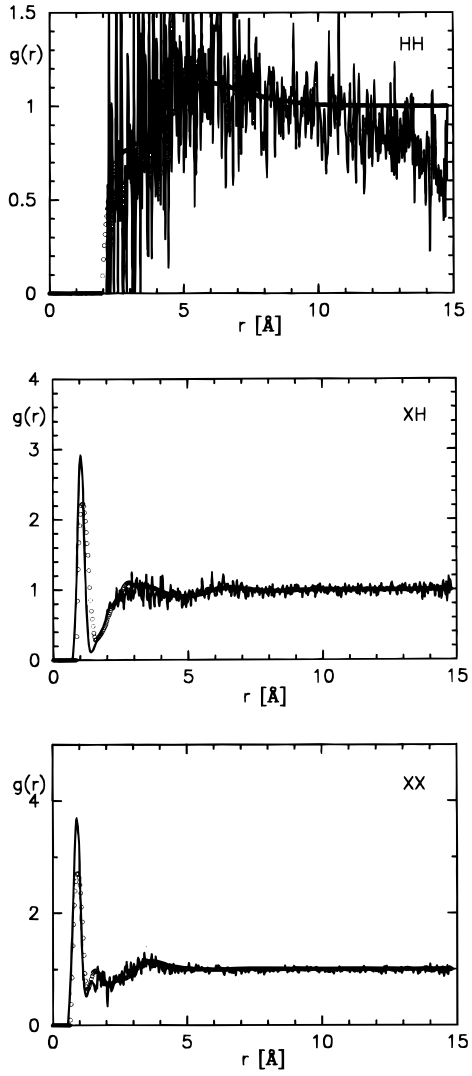

Figure 4. EPSR "fits" (derived from a single configuration of 250 molecules: 15 tertiary butanol molecules and 235 water molecules) to the experimental partial distribution functions for 0.06 mole fraction tertiary butanol in water, $g_{HH}(r)$, $g_{XH}(r)$, and $g_{XX}(r)$. (—) EPMC fit; (○) experimental data.

latter function is more informative than the partial pair distribution functions for describing the structure in a molecular liquid[7] since it relates the relative position vector, **r**, of two molecules, 1 and 2, with their orientations ω_1 and ω_2 in the laboratory reference frame.

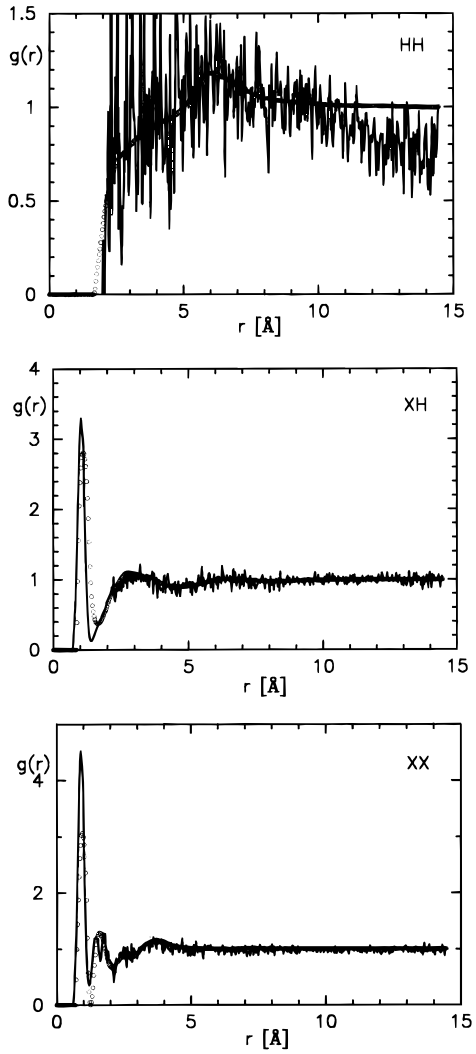

Figure 5. EPSR "fits" (derived from a single configuration of 200 molecules: 22 tertiary butanol molecules and 178 water molecules) to the experimental partial distribution functions for 0.11 mole fraction tertiary butanol in water, $g_{HH}(r)$, $g_{XH}(r)$, and $g_{XX}(r)$: (—) EPMC fit; (○) experimental data.

The orientational pair correlation function can be expanded as a series of spherical harmonic coefficients,[8] $h(l_1l_2l;n_1n_2;r)$, where l_1, l_2, n_1, n_2 relate to the orientational coordinates ω_1 and ω_2 while l relates to the spatial distribution of molecule 2 about molecule 1. This expansion is especially useful because once the coefficients have been determined, they can be used to reconstruct $g(\mathbf{r},\omega_1,\omega_2)$ over any specified region of parameter space, without the need to run the computer simulation again. In this work the spherical harmonic coefficients were generated from the configurations of molecules determined in the empirical potential structure refinement.

C. EPSR Model Initialization: Tertiary Butanol in Water. Simulation boxes containing 15 tertiary butanol molecules and 235 water molecules, 22 tertiary butanol molecules and 178 water molecules, and thirdly 32 tertiary butanol molecules and 168 water molecules were generated to model the 0.06, 0.11, and 0.16 mole fraction data, respectively. The box dimensions corresponding to each of these concentrations are 21.108, 20.643, and 21.594 Å, respectively. The structural information on the modeled system is extracted as an ensemble average over many thousands of configurations which involve $\approx 2 \times 10^7$ atom or molecule moves. The EPSR procedure allows for four types of "moves" which are individual atom

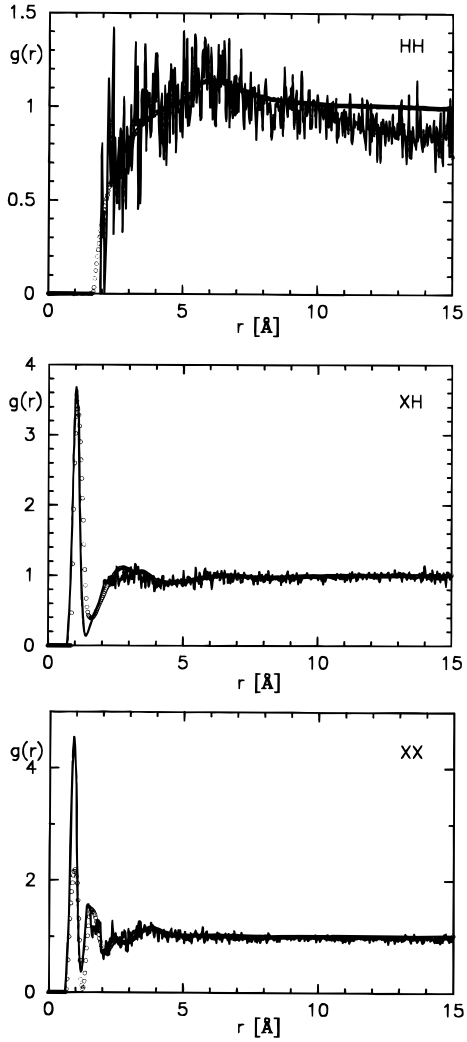

Figure 6. EPSR "fits" (derived from a single configuration of 200 molecules: 32 tertiary butanol molecules and 168 water molecules) to the experimental partial distribution functions for 0.16 mole fraction tertiary butanol in water, $g_{HH}(r)$, $g_{XH}(r)$, and $g_{XX}(r)$: (—) EPMC fit; (○) experimental data.

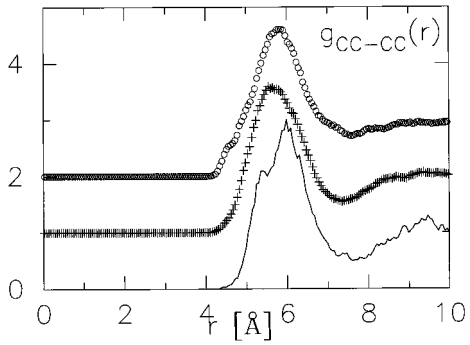

Figure 7. Tertiary butanol−tertiary butanol molecular centers functions evaluated for 0.06, 0.11, and 0.16 mole fraction alcohol in water: (○) 0.16 mole fraction alcohol in water; (+) 0.11 mole fraction alcohol in water; (—) 0.06 mole fraction alcohol in water. Functions are offset vertically for clarity.

translations, functional group rotation on a molecule, whole molecule translations, and finally whole molecule rotations. In this manner a comprehensive range of structural configurations is generated. The interatomic potentials used to seed these simulations were, for the alcohol molecules, the OPLS potentials of Jorgensen et al.[10,11] and, for water, the SPC/E potentials of Berendsen et al.[12] These potentials were chosen to provide a reasonable starting point from which to model these systems, as the intermolecular hydrogen bonding correlations in the solvent are only weakly weighted in the measured experimental composite distribution functions (see Table 1). In addition, internal molecular geometry is preserved in EPSR by introducing suitable harmonic forces between atoms in the same molecule. It should be noted that these potentials are used only to seed the EPSR model. Once refinement has begun, perturbations to these potentials are added within the constraints imposed by the measured partial distribution functions.

It is important to emphasize that the EPSR procedure does not vary the parameters that characterize the seed potentials. Instead the method proceeds by adding an empirically derived perturbation potential to these starting potentials. The perturbation is derived from the ratio of measured to calculated radial distribution functions (eq 14); see ref 6 for details. For the present case, two of the measured radial distribution functions are in fact composite (XH, XX), consisting of several individual site−site terms added together with the weightings shown in Table 1. Therefore the empirical potentials derived from these data sets are also composite, representing averages of the corresponding site−site potentials. Since these empirical perturbations are complicated functions of r, attempts to parametrize them in terms of familiar quantities uch as Lennard-Jones parameters and partial atomic charges have not been successful.

Given these facts, the actual potentials used to seed the modeling process are not believed to be fundamentally important to the outcome. Their selection criteria is only that they provide a reasonable starting point and structure from which the EPSR-derived perturbation functions can be generated. In the present experiment, which involved hydrogen isotope substitution *only* on the TBA molecules, it was essential to use a seed potential that would generate at least qualitatively correct hydrogen-bonded configurations of water molecules. Because direct information on the water−water correlations was not available in the present experiment, the results are sensitive primarily to alcohol−alcohol correlations.

IV. Results

A. Experiment. Figures 1−3 show the partial structure factors $S_{HH}(Q)$, $S_{XH}(Q)$, and $S_{XX}(Q)$ for 0.06, 0.11, and 0.16 mole fraction tertiary butanol in water, respectively. For clarity, the displayed Q range is 0−15 Å^{-1}, although useful data were collected out to ≈40 Å^{-1}. These functions have been corrected for residual low-frequency background components remaining after the standard data analysis procedures, by forcing the calculated radial distribution function to be zero below a specified minimum radius. The data were then converted to real space by using a minimum noise Fourier transform procedure.[9] This, in turn, led to the composite radial distribution functions shown as the experimental data (circles) in Figures 4−6. The intermolecular partial structure factors $S_{HH}(Q)$ and partial distribution functions $g_{HH}(r)$ arise from the intermolecular structural correlations between the methyl hydrogens of the tertiary butanol molecules in the solutions. Any intramolecular correlations between these methyl hydrogen sites contribute to the composite $S_{XH}(Q)$ and $g_{XH}(r)$ functions as in-solution isotopic exchange between methyl group hydrogen or deuterium does not take place. The relatively featureless shape of $g_{HH}(r)$ arises predominantly from the high degree of distance averaging that occurs due to the large spatial extent of the methyl hydrogens on the alcohol molecules and also reflects the wide range of

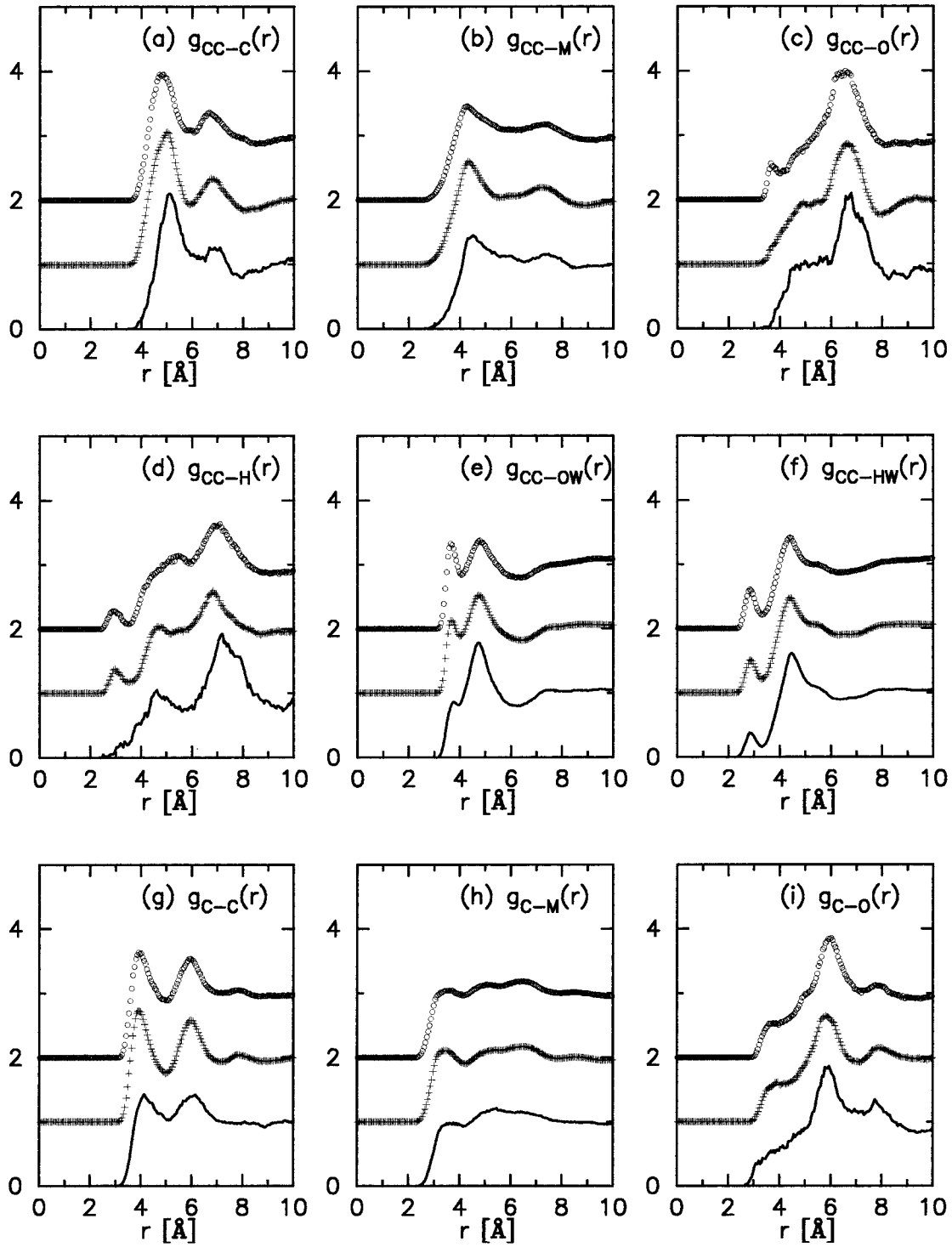

Figure 8. Intermolecular partial distribution functions 1: CC−C, CC−M, CC−O, CC−H, CC−OW, CC−HW, C−C, C−M, C−O, for 0.06, 0.11, and 0.16 mole fraction tertiary butanol in water: (○) 0.16 mole fraction alcohol in water; (+) 0.11 mole fraction alcohol in water; (—) 0.06 mole fraction alcohol in water. Functions are offset vertically for clarity.

intermolecular configurations that exists between the molecules. The composite partial pair distribution functions $g_{XH}(r)$ and $g_{XX}(r)$ are difficult to interpret directly due to the large number of inter- and intramolecular atomic correlations from which they are derived.

B. EPSR Modeling. As well as showing the HH, XH, and XX radial distribution functions derived from the diffraction data, Figures 4−6 show the equivalent EPSR-generated pair distribution functions as calculated from a single configuration of molecules. Because of the small number of alcohol molecules involved in these simulations and the fact that the plotted curves sampled only one configuration, the simulated distributions necessarily appear very noisy here. However the subsequent ensemble averaging that took place over several thousand configurations ensured that the average radial distribution functions, as shown in Figures 7−10, and the calculated spherical harmonic coefficients used in Figures 12−14 were indeed quite smooth.

Nonetheless, it can be seen that over the range for which the simulated $g(r)$s are strictly valid (namely half the box size, or

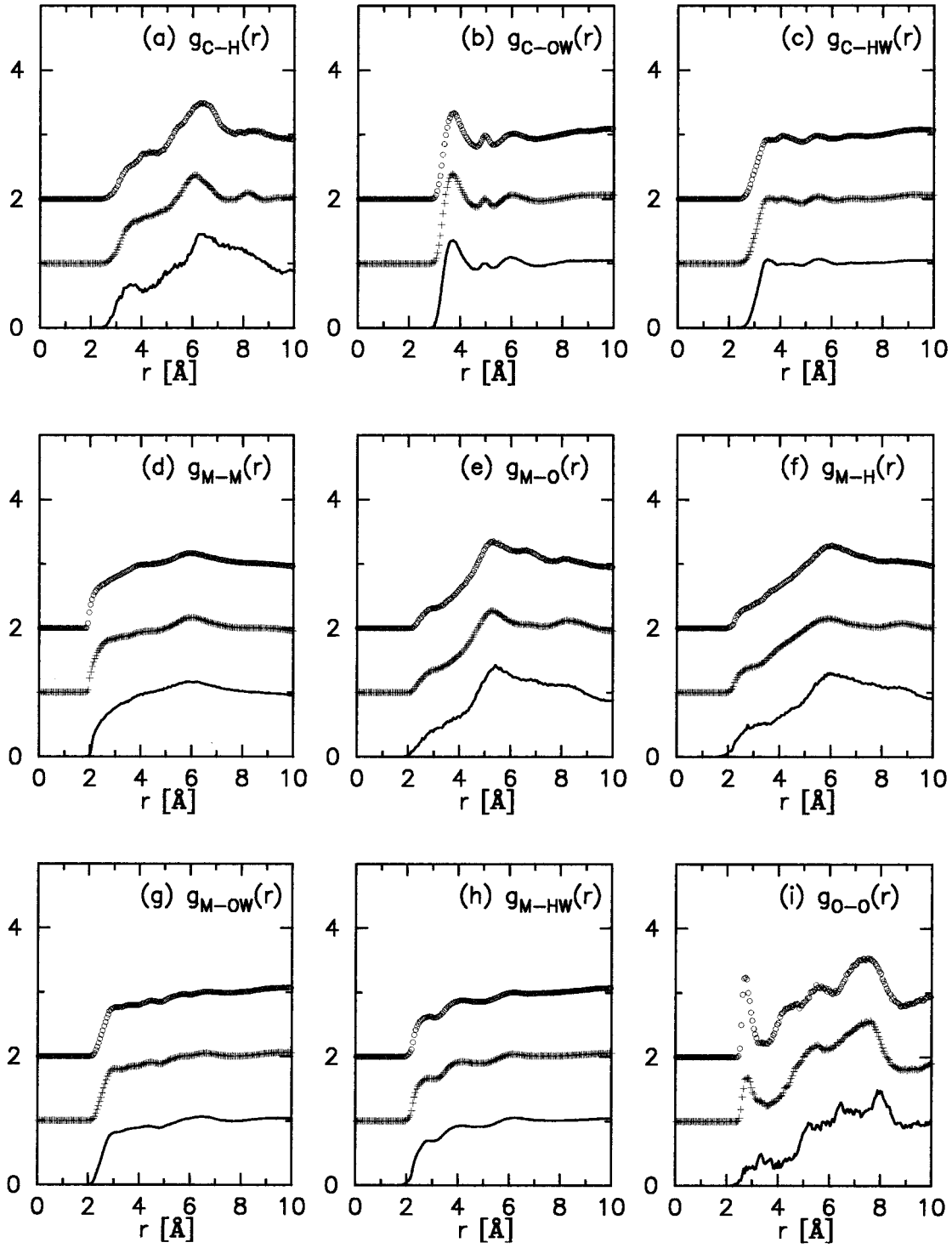

Figure 9. Intermolecular partial distribution functions 2: C−H, C−OW, C−HW, M−M, M−O, M−H, M−OW, M−HW, O−O, for 0.06, 0.11, and 0.16 mole fraction tertiary butanol in water: (○) 0.16 mole fraction alcohol in water; (+) 0.11 mole fraction alcohol in water; (−) 0.06 mole fraction alcohol in water. Functions are offset vertically for clarity.

$r \leq 10$ Å), the general level of agreement with the experimental distribution functions is quite good, even though some discrepancies still occur (see discussion in section V below). In particular, that the agreement seen here was much better than obtained if the simulations were run with the seed potentials on their own, was demonstrated in the early part of the simulations.

The alcohol−alcohol molecular centers functions and the remaining intermolecular partial pair distribution functions are shown in Figures 7−10. The atomic site labeling system is

CC tertiary butanol central carbon

C tertiary butanol methyl group carbon

M tertiary butanol methyl group hydrogen

O tertiary butanol hydroxyl group oxygen

H tertiary butanol hydroxyl group hydrogen

OW water molecule oxygen

HW water molecule hydrogen

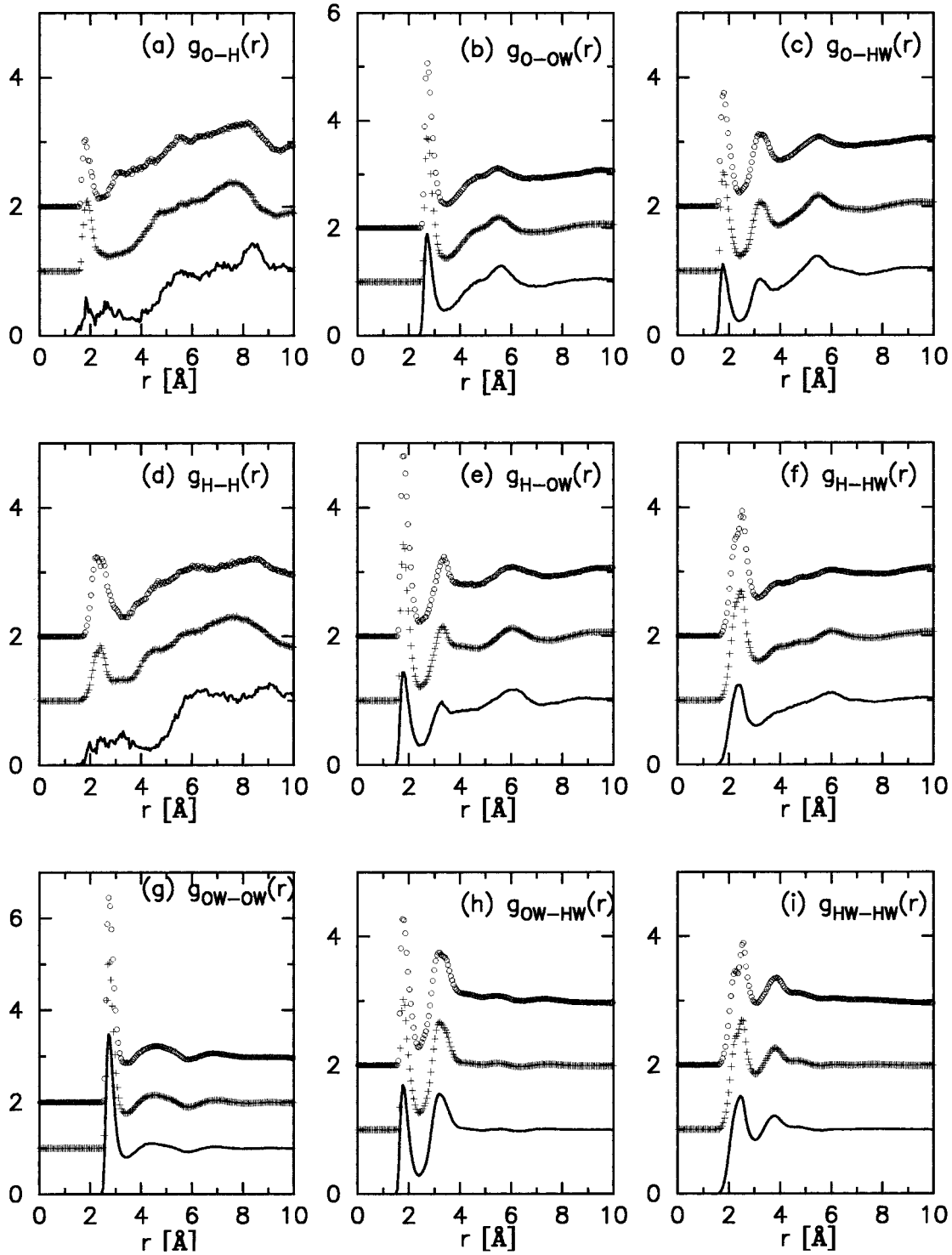

Figure 10. Intermolecular partial distribution functions 3: O−H, O−OW, O−HW, H−H, H−OW, H−HW, OW−OW, OW−HW, HW−HW, for 0.06, 0.11, and 0.16 mole fraction tertiary butanol in water; (○) 0.16 mole fraction alcohol in water; (+) 0.11 mole fraction alcohol in water; (—) 0.06 mole fraction alcohol in water. Functions are offset vertically for clarity.

The relative contributions of each of these partial distribution terms to the experimentally measured HH, XH, and XX partial distribution functions are given in Table 1.

C. Spherical Harmonic Analysis. Figures 11−14 relate to the intermolecular orientational correlations between solute alcohol molecules. Figure 11 shows the coordinate system between two tertiary butanol molecules, by which Figures 12−14 are defined. Figures 12−14 each consists of four correlation plots corresponding to (A) the positions of neighboring alcohol molecule centers around any arbitrarily chosen molecule as a function of θ_l and averaging over all the other angular parameters, ϕ_l, θ_m, ϕ_m, and χ_m; (B) the relative orientation of a neighboring molecule in the direction of $\theta_l = 0°$ (corresponding to molecules in the brightest lobe in Figures 12a, 13a, and 14a); the map is plotted as a function of θ_m with all other angular parameters averaged; (C) the relative orientation of a neighboring molecule in the direction $\theta_l = 75°$, i.e. molecular approach predominantly in the direction of the methyl groups of a central alcohol molecule; again this plot is as a function of θ_m, but with $\phi_m = 0°$, and averaging over the remaining angular

TABLE 2: Coordination Numbers Obtained from Integration of the Features in the CC−CC, CC−OW, CC−HW, O−OW, O−HW, H−OW, H−HW, O−O, O−H, and H−H Partial Distribution Functions for 0.06, 0.11, and 0.16 Mole Fraction Tertiary Butanol in Water

correlation	R_{min} (Å)	R_{max} (Å)	$\rho_{0.06}$ (atom Å^{-3})	C.N.(0.06) (atoms)	$\rho_{0.11}$ (atom Å^{-3})	C.N.(0.11) (atoms)	$\rho_{0.16}$ (atom Å^{-3})	C.N.(0.16) (atoms)
CC−CC	4.0	7.0	0.00161	2.8 ± 0.6	0.00255	4.4 ± 0.6	0.00325	5.8 ± 0.6
CC−OW	3.0	4.0	0.0253	2.1 ± 0.4	0.0206	2.2 ± 0.3	0.0171	2.0 ± 0.2
	4.0	6.2		21.0 ± 1.2		16.4 ± 0.9		12.8 ± 0.6
	3.0	6.2		23.1 ± 1.2		18.7 ± 0.9		14.8 ± 0.7
CC−HW	2.3	3.25	0.0505	1.1 ± 0.3	0.0412	1.2 ± 0.2	0.0341	1.1 ± 0.2
	3.25	5.0		21.0 ± 1.2		16.4 ± 0.9		13.1 ± 0.6
	3.25	6.0		41.5 ± 1.7		32.3 ± 1.2		25.4 ± 0.9
	5.0	6.0		20.5 ± 1.2		15.9 ± 0.9		12.3 ± 0.6
O−OW	2.3	3.3	0.0253	2.2 ± 0.4	0.0206	2.3 ± 0.3	0.0171	2.1 ± 0.3
O−HW	1.4	2.5	0.0505	1.2 ± 0.3	0.0412	1.3 ± 0.2	0.0341	1.2 ± 0.2
	2.5	4.0		7.1 ± 0.7		6.6 ± 0.6		5.6 ± 0.4
H−OW	1.4	2.5	0.0253	0.84 ± 0.23	0.0206	0.9 ± 0.2	0.0171	0.86 ± 0.16
	2.5	4.0		4.0 ± 0.5		3.6 ± 0.4		2.9 ± 0.3
H−HW	1.5	3.0	0.0505	3.8 ± 0.5	0.0412	3.9 ± 0.4	0.0341	3.6 ± 0.3
O−O	2.4	3.25			0.00255	0.12 ± 0.10	0.00325	0.2 ± 0.1
O−H	2.5	3.5			0.00255	0.07 ± 0.07	0.00325	0.06 ± 0.06
H−H	1.6	3.0			0.00255	0.17 ± 0.11	0.00325	0.3 ± 0.1

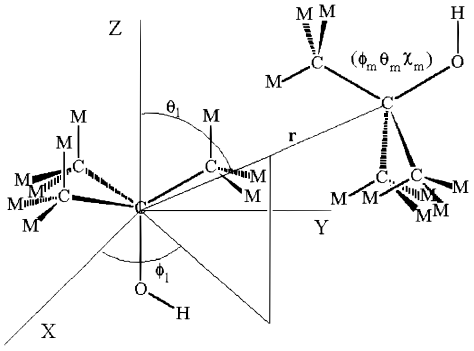

Figure 11. Schematic diagram of the coordinate system used to define the orientational correlations between tertiary butanol molecules.

coordinates; (D) the final correlation map, probing the intermolecular correlations in a region close to the hydroxyl group on the central tertiary butanol molecule, $\theta_l = 135°$; again this is plotted as a function of θ_m with $\phi_m = 0°$ and other angular components averaged out.

V. Discussion

As already described above, the EPSR-generated distributions derived from the experimentally determined HH, XH, and XX pair distribution functions shown in Figures 4−6 are seen to show sensible agreement with the data in the range 0−10 Å, after account is taken of the large statistical noise implicit in one configuration of a relatively dilute system. Beyond this distance range the calculated HH distribution is seen to deviate from the target level of $g_{HH}(r) = 1.0$ at large r. This is apparently due to a clustering of alcohol molecules within the simulation box, where the restriction to a finite box size and finite number of molecules results in an inability to model the more distant intermolecular correlations correctly. This deviation from the constraining data is unlikely to influence significantly the structural correlations being studied in the shorter distance range of 0−10 Å. In addition it should be borne in mind that due to the truncation of the diffraction data at low-Q, the experimental $g(r)$s are themselves not reliable much beyond this distance range.

The observation of clustering between alcohol molecules in aqueous solution in the EPSR simulation is an intriguing phenomenon. Obviously it might always be an artifact of the box size and other inadequacies of the simulation, but it is consistent with existing light scattering[13−16] and X-ray scattering[17,18] data in the literature, which provides clear evidence that for alcohol concentrations above about 0.04 mole fraction in the tertiary butanol−water system molecular association is present. It is interesting to note that these mesoscopic effects would be more visible in a small angle neutron scattering experiment, below the minimum scattering vector used in the current data analysis.

Comparison of simulated and experimental XH and XX partial distribution functions shows the poorest agreement in the short-range, intramolecular correlation region. This is partly due to the difficulty of accurately modeling the intramolecular correlations in the tertiary butanol and water molecules with rigid molecules. In principle provision is made within the EPSR technique for a harmonic energy parameter to be defined that governs the vibrational motion of the atomic sites on each molecule. At the time of the simulations described here however it proved nontrivial to apply this parameter in a manner that did not lead to an excessively distorted molecular geometry. Therefore for the present simulations the intramolecular vibrational motion was kept tightly constrained, although relatively free rotational motions of the functional groups on the alcohol molecule were permitted, and the observed broadening of the intramolecular peaks was simulated with a Gaussian function of the appropriate width.

A second feature that contributes to the lack of fit at low r is that the measured diffraction data frequently have a residual background term slowly varying with Q which is a consequence of incomplete or inaccurate subtraction of the inelasticity effects. Such a background, if present, produces a distortion at low r, which has generally disappeared for radius values that correspond to intermolecular correlations ($r > 2$ Å). It is difficult to remove this bias from the structure data without also losing important intermolecular structural information, so in this work we have chosen to leave the background in the data. The tight constraints on the molecular geometries used here ensured that the simulation proceeded with realistic models of the water and tertiary butanol molecules, while giving sensible fits in the important intermolecular region. Future work with the EPSR technique is likely to involve fitting directly in Q space, which will clarify better the distinction between intramolecular structure and residual inelasticity effects.

For these reasons we believe that the EPSR-generated intermolecular correlation functions derived from the data of these experiments are a realistic description of the structure of these solutions.

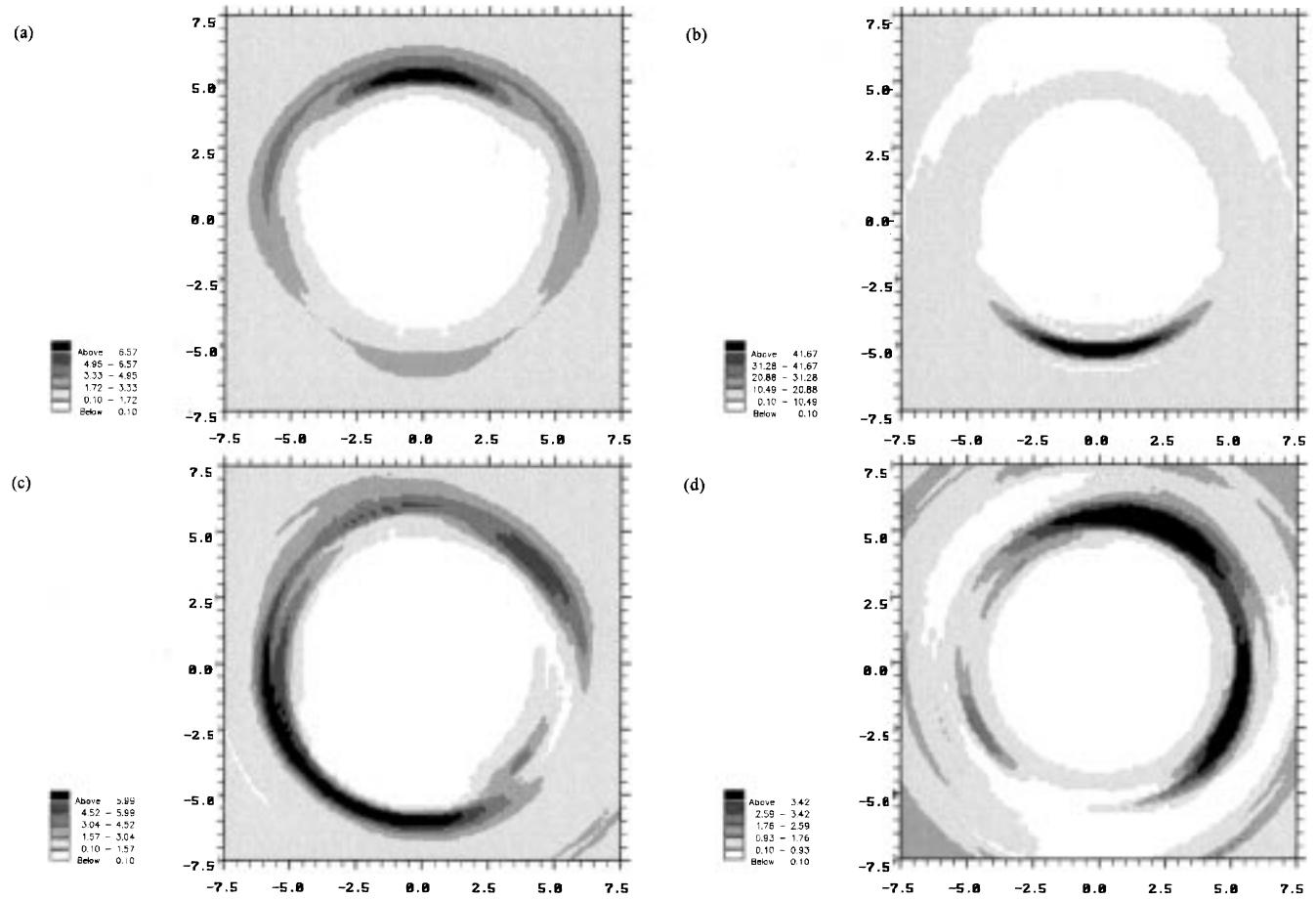

Figure 12. (a) Orientational distribution map of tertiary butanol molecular centers in 0.06 mole fraction aqueous solution as a function of θ_l, averaging over the remaining molecular orientations, i.e. $\langle\phi_l\rangle$, $\langle\phi_m\rangle$, $\langle\theta_m\rangle$, and $\langle\chi_m\rangle$. (b) Orientational distribution map of tertiary butanol molecular centers in 0.06 mole fraction aqueous solution as a function of θ_m with $\theta_l = 0°$ and averaging over the remaining molecular orientations, i.e. $\langle\phi_l\rangle$, $\langle\phi_m\rangle$, and $\langle\chi_m\rangle$. (c) Orientational distribution map of tertiary butanol molecular centers in 0.06 mole fraction aqueous solution as a function of θ_m with $\theta_l = 75°$ and $\phi_m = 0°$ and averaging over the remaining molecular orientations, i.e. $\langle\phi_l\rangle$ and $\langle\chi_m\rangle$. (d) Orientational distribution map of tertiary butanol molecular centers in 0.06 mole fraction aqueous solution as a function of θ_m with $\theta_l = 135°$ and $\phi_m = 0°$ and averaging over the remaining molecular orientations, i.e. $\langle\phi_l\rangle$ and $\langle\chi_m\rangle$.

A. Centers Correlations. An examination of the centers partial distribution functions determined by the data modeling process shows them to be broadly similar for the three concentrations, but with several significant differences. The solute−solute molecular centers function (CC−CC) shown in Figure 7 shows, for the 0.06 mole fraction alcohol solution, a single peak between 4.0 and 7.0 Å, with an area that corresponds to approximately 2.8 ± 0.6 alcohol centers (Table 2). This is indicative that, on average, trimer solute aggregate configurations are favored in aqueous solutions of this concentration, though dimer and tetramer configurations cannot be excluded. The solute−solute molecular centers functions for the 0.11 and 0.16 mole fraction solutions again have single peaks between 4.0 and 7.0 Å; this feature is slightly shifted from that found in the more dilute system. In the higher concentration solutions there is a corresponding increase in the solute−solute coordination numbers to 4.4 ± 0.6 and 5.5 ± 1.3 direct solute−solute contacts for the 0.11 and 0.16 mole fraction concentration systems respectively (Table 2). None of the CC−CC partial distribution functions show evidence for a second solute−solute coordination shell, although the lowest concentration system shows a distinct shoulder on the rising edge of the centers peak, which is reminiscent of that observed in pure tertiary butanol data where it corresponded to hydrogen-bonded configurations betweenalcohol molecules.[21] However, in the 0.06 mole fraction aqueous system, this rising edge feature occurs at ≈5.3 Å rather than ≈4.8 Å, as found in the pure liquid alcohol, and the orientational correlation analysis (see below) shows this feature to correlate with strong intermolecular methyl group to methyl group correlations.

B. CC−OW and CC−HW Correlations. The solute hydration is perhaps best illustrated through the CC−OW partial distribution function (Figure 8). In the 0.06 mole fraction system, this partial shows a main peak at 4.8 Å, with a shoulder at 3.6 Å. In the higher concentration solutions, this partial distribution function clearly separates the solute−solvent correlations into two components at 3.6 and 4.8 Å. Integration of these partial distribution functions to obtain hydration numbers of the solute molecules yields 2.1 ± 0.4 water oxygens at a distance between 3.0 and 4.0 Å and 21.0 ± 1.2 water oxygens between 4.0 and 6.2 Å in the 0.06 mole fraction solution, 2.2 ± 0.3 and 16.4 ± 0.9 water oxygens in the 0.11 mole fraction system, and 2.0 ± 0.2 and 12.8 ± 0.6 water oxygens in the 0.16 mole fraction solution (Table 2). Thus the shorter range correlations which correspond to water molecules hydrogen bonded to the hydroxyl group of the alcohol are constant over the investigated concentration range, and changes in hydration structure occur only in the remainder of the alcohol hydration

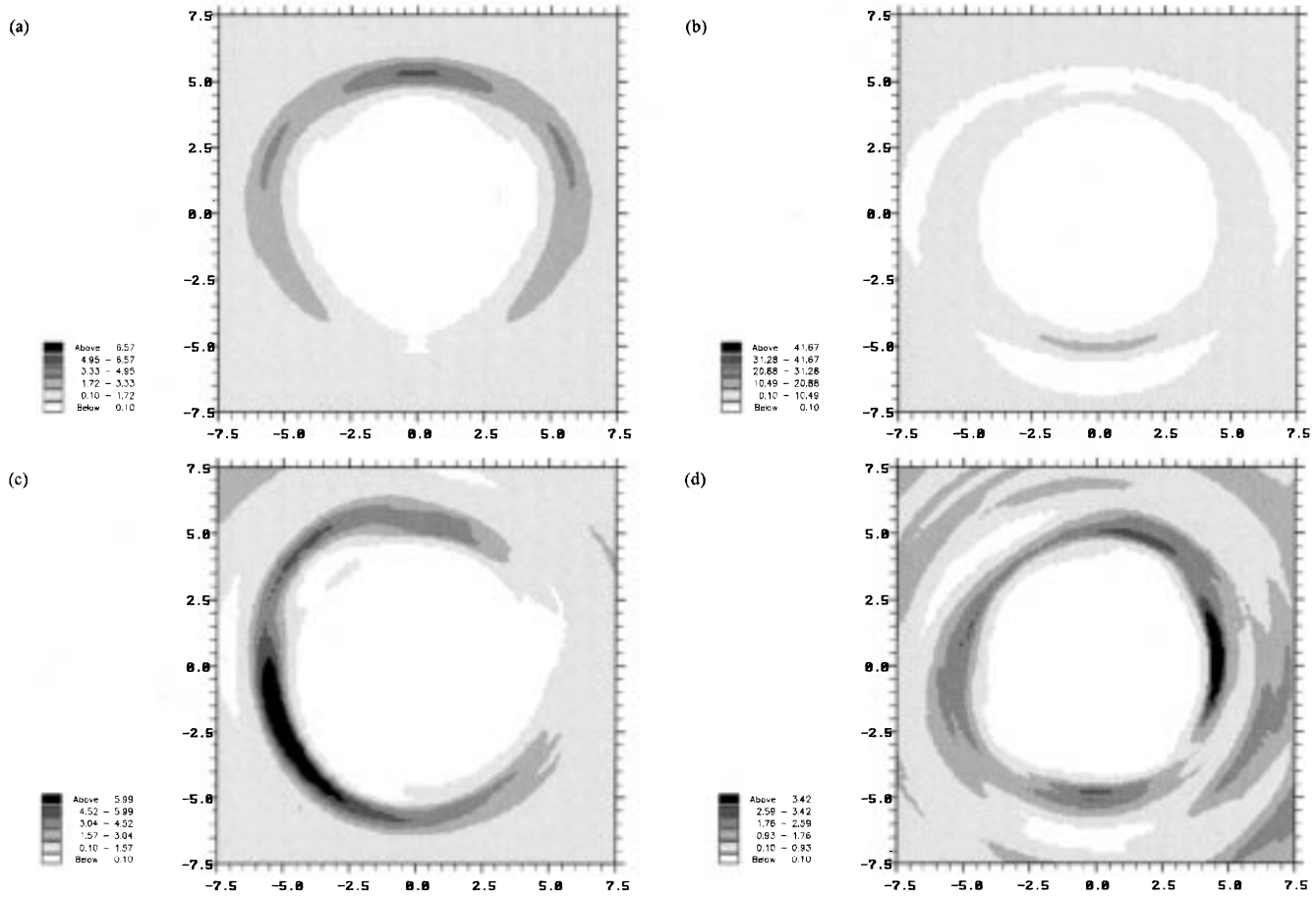

Figure 13. Solute−solute orientational distribution maps for tertiary butanol in 0.11 mole fraction aqueous solution. Angular dependencies as found in Figure 12.

shell, as shown by the decrease in the number of water molecules contributing to the second feature in the partial distribution functions at 4.8 Å.

The hydration of the nonpolar methyl groups, although not highly weighted in the experimental data used to constrain the modeling process, can be investigated through the M−OW and M−HW partial distribution functions (Figure 9). The fact that the initial rise of both the oxygen and hydrogen functions occurs at about the same distance is consistent with other work suggesting that the water dipoles tend to be preferentially oriented tangential to a sphere centered on the methyl carbon.[22] The broad similarity between these two functions suggests there is no dominating intermolecular orientational preference apart from this.

C. Water Partial Distribution Functions. The OW−OW, OW−HW, and HW−HW partial distribution functions (Figure 10) are as would be expected for water. The majority of the constraints on these partial distribution functions arise from the use of the SPC/E parameters in the initial seeding of the model. The unexpected feature in the slight splitting of the first HW−HW peak for the 0.16 mole fraction system is difficult to justify in the absence of directly constraining experimental data relating to the water structure. It may be a model-dependent artifact induced by the small number of water molecules in the simulation box, and it may be coupled with the self-association phenomena manifest between the alcohol molecules. Further experiments are under way that will clarify this point.

D. Solute−Solute Intermolecular Orientational Correlations. A comparison between Figures 12a, 13a, and 14a shows that there is a reduction in intensity in the correlation lobe at $\theta_l = 0°$ (12 o'clock on the figures) as the concentration of tertiary butanol is increased from 0.06 to 0.16 mole fraction. This dark (high-intensity) lobe in Figure 12a (and the corresponding reduced intensity lobes in Figures 13a and 14a) is relatively close in and corresponds to the rising edge feature in the 0.06 mole fraction molecular centers $g(r)$ (CC−CC) (Figure 7). The majority of the molecular centers correlation is contained in the more diffuse regions of Figures 12a, 13a, and 14a. Figures 12b, 13b, and 14b, clearly show that the relative orientation of a tertiary butanol that approaches the arbitrary central molecule in the $\theta_l = 0°$ direction would favor methyl group to methyl group contacts. The strength of this orientational correlation is strongest in the 0.06 mole fraction system, as evidenced by the magnitude of the correlations in the lobe (at 6 o'clock). The 0.11 mole fraction system shows the widest range of methyl group to methyl group contacts, but by 0.16 mole fraction solute concentration, the tendency for fairly direct methyl group to methyl group contacts is restored, although at a lower intensity than in the 0.06 mole fraction system. Figures 12c, 13c, and 14c show that the tendency for methyl group to methyl group contacts persists at $\theta_l = 75°$ (the lobes in the region of 7 o'clock), although there is some evidence for methyl group to hydroxyl group correlations between neighboring alcohol molecules in this region, particularly in the 0.06 mole fraction case (the lobe at 2 o'clock). The broader distribution of features relating to nonpolar to nonpolar group contacts in the 0.16 mole fraction solution illustrates that as the solute concentration increases, an increased range of such molecular contacts is required and is comparable with the distribution found in the pure liquid alcohol.[21]

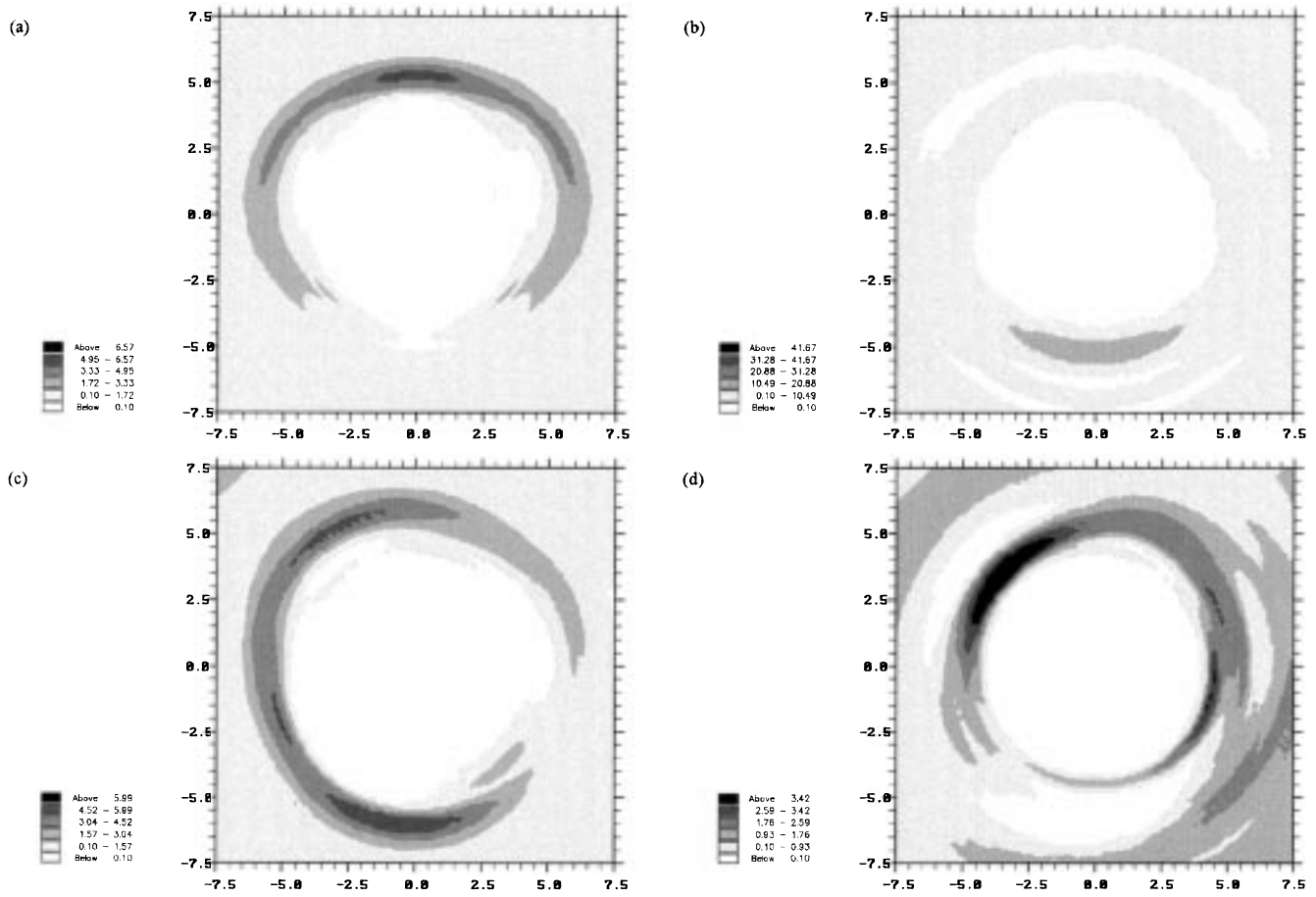

Figure 14. Solute−solute orientational distribution maps for tertiary butanol in 0.16 mole fraction aqueous solution. Angular dependencies as found in Figure 12.

Figures 12d, 13d, and 14d show that in the $\theta_l = 135°$ direction a range of configurations involving methyl and hydroxyl group contacts is present over the investigated concentrations. In the 0.06 mole fraction system, there is evidence that hydrogen-bonded hydroxyl group−hydroxyl group correlations are favored in the region of high intensity at 4 o'clock in Figure 12d (albeit at a very low probability, as indicated by an examination of the $\theta_l = 135°$ region of Figure 12a (at 4 o'clock). By comparison, contacts in this region at 0.16 mole fraction concentration would favor a methyl group approach to the hydroxyl group of an arbitrarily chosen central molecule, a polar to nonpolar group interaction (as evidenced in the high intensity of the lobes at 11 o'clock in Figure 14d). The case for the 0.11 mole fraction system is found to be transitional between the lower and higher concentration solutions, with a mixture of hydrogen bonding and polar to nonpolar interactions. This observation can be placed in context when comparing with results obtained for a pure tertiary butanol system.[21] In the pure solvent, hydrogen-bonded correlations between the hydroxyl groups of neighboring alcohol molecules are found to be strong, with one such hydrogen bond per alcohol molecule. However, there is found to be an equal relative intensity of methyl group to hydroxyl group interactions in the $\theta_l = 135°$ region as found in the 0.16 mole fraction aqueous solution. This indicates that one of the dominant distinguishing features of the aqueous systems in comparison to the pure alcohol system is the "satisfaction" of the alcohol hydrogen-bonding requirements by the available water, with the level of nonpolar to polar correlations between alcohol molecules appearing to reach the level found in the pure alcohol case by 0.16 mole fraction concentration. These conclusions are of interest for our understanding of the hydrophobic interactions between these molecules. As mentioned in the literature on tertiary butanol−water solutions,[1] the greatest deviations from ideal liquid mixture behavior are observed at a concentration of 0.04 mole fraction. These nonideal mixing effects are believed to be due to hydrophobic processes. Consistent with this view, the intermolecular solute−solute correlations in the 0.06 mole are best suited to the study of hydrophobically driven molecular interactions. Clearly, the straight ($\theta_l = 0°$) intermolecular methyl group to methyl group correlation dominates at this concentration.

This interaction remains strong at the higher concentrations, although a wider range of molecular contacts becomes evident. Over the entire range of concentrations studied here, the hydrogen-bonding requirements of the alcohol hydroxyl groups are fully satisfied by the available water molecules, although by 0.16 mole fraction, the intermolecular orientational correlations begin to resemble those found in the pure liquid alcohol,[21] except for the absence of alcohol−alcohol hydrogen bonds.

VI. Conclusions

The results outlined above support a model for aqueous solutions of tertiary butanol (> 0.04 mole fraction) in which the majority of association of the alcohol molecules is through their nonpolar methyl group regions rather than via polar (presumably hydrogen-bonding) interactions of their hydroxyl groups, most obviously at the lower concentration of 0.06 mole fraction alcohol in water. This model is consistent with results of an earlier Monte Carlo simulation study of 0.03 mol % tertiary butanol in water,[20] which found no evidence for

hydrogen-bonding interactions between the alcohol molecules. From the data presented here—particularly the geometrical configurations determined from the orientational correlation maps—evidence for hydrogen bonding between the alcohol molecules is absent, even in the 0.16 mole fraction concentration system. The quantity of water molecules in the solution over the investigated concentration range is sufficient to satisfy the expected hydrogen-bonding requirements of the alcohol molecule hydroxyl groups.

The relative strengths of the orientational correlations mapped in Figures 12−14 indicate that this direct methyl group contact is dominant over the majority of the parameter space probed by the experiment. In the (lower concentration) Monte Carlo simulation study[20] some evidence was found for the coexistence of solvent-separated and direct contact configurations, but a more recent simulation study of an ethanol-water system[23] suggests that even in extremely dilute systems direct solute association is the preferred mixing state, and it can be inferred from the results presented here that by a concentration of 0.06 mole fraction all close solute−solute contacts are direct.

The molecular centers distribution functions at all three concentrations are similar. They all display a single feature at approximately 5.5 Å, which is indicative of direct alcohol molecule contact. This result suggests that models in which aggregates of clathrate-like alcohol hydrates are present in the mixture beyond 0.04 mole fraction[13,17,18] may require revision. It should however be remembered that even at the lowest concentration studied here the tertiary butanol molecule is sufficiently large so as to make complete water encapsulation of each alcohol molecule unlikely.

Acknowledgment. We would like to thank the Engineering and Physical Sciences Research Council (EPSRC), U.K., for funding under Grant GR/K/12465, and the Council for the Central Laboratory of Research Councils for access to their neutron facility, ISIS, Rutherford Appleton Laboratory, Oxfordshire, U.K.

References and Notes

(1) Franks, F.; Desnoyers, J. E. *Water Sci. Rev.* **1985**, *1*, 1.
(2) Franks, F.; Ives, D. J. G. *Q. Rev. Chem. Soc.* **1966**, *20*, 1.
(3) Blokzijl, W.; Engberts, J. B. F. N. *Angew. Chem. Intl. Ed. Engl.* **1993**, *32*, 1545.
(4) Soper, A. K.; Howells, W. S.; Hannon, A. C. *ATLAS−Analysis of Time-of-Flight Diffraction Data from Liquid and Amorphous Samples*; Rutherford Appleton Laboratory Report RAL 89-046, 1989.
(5) Soper, A. K.; Luzar, A. *J. Chem. Phys.* **1992**, *97*, 1320.
(6) Soper, A. K.; *Chem. Phys.* **1996**, *202*, 295.
(7) Soper, A. K. *J. Chem. Phys.* **1994**, *101*, 6888.
(8) Gray, C. G.; Gubbins, K. E. *Theory of Molecular Fluids Volume 1: Fundamentals*; Clarendon Press: Oxford, 1984.
(9) Soper, A. K. *Neutron Scattering Data Analysis 1990*; Johnson, M. W., Ed.; IOP Conference Series Number 107; IOP Publishing: Bristol, 1990; p 57.
(10) Jorgensen, W. L.; Madura, J. D.; Swenson, C. J. *J. Am. Chem. Soc.* **1984**, *106*, 6638.
(11) Jorgensen, W. L. *J. Phys. Chem.* **1986**, *90*, 1276.
(12) Berendsen, H. J. C.; Grigera, J. R.; Straatsma, T. P. *J. Phys. Chem.* **1987**, *91*, 6269.
(13) Iwasaki, K.; Fujiyama, T. *J. Phys. Chem.* **1977**, *81*, 1908.
(14) Iwasaki, K.; Fujuyama, T. *J. Phys. Chem.* **1979**, *83*, 463.
(15) Euliss, G. W.; Sorensen, C. M. *J. Chem. Phys.* **1984**, *80*, 4767.
(16) Bender, T. M.; Pecora, R. *J. Phys. Chem.* **1986**, *90*, 1700.
(17) Nishikawa, K.; Hayashi, H.; Iijima, T. *J. Phys. Chem.* **1989**, *93*, 6559.
(18) Nishikawa, K.; Kodera, Y.; Iijima, T. *J. Phys. Chem.* **1987**, *91*, 3694.
(19) Narten, A. H.; Sandler, S. I. *J. Chem. Phys.* **1979**, *71*, 2069.
(20) Tanaka, H.; Nakanishi, K.; Touhara, H. *J. Chem. Phys.* **1984**, *81*, 4065.
(21) Bowron, D. T.; Finney, J. L.; Soper, A. K. *Mol. Phys.* **1998**, *93*, 531.
(22) Soper, A. K.; Finney, J. L. *Phys. Rev. Lett.* **1993**, *71*, 4346.
(23) Nishi, N.; Takahashi, S.; Matsumoto, M.; Tanaka, A.; Muraya, K.; Takamuku, T.; Yamaguchi, T. *J. Phys. Chem.* **1995**, *99*, 462.